Configurational lattice dynamics: The phase diagram of Rh-Pd

C. Cienfuegos,[1] E. P. Isoardi,[2] and G. D. Barrera[1]
[1]*Departamento de Química, Universidad Nacional de la Patagonia SJB, Ciudad Universitaria, (9000) Comodoro Rivadavia, Argentina*
[2]*Departamento de Química Inorgánica, Analítica y Química Física, Facultad de Ciencias Exactas y Naturales, Universidad de Buenos Aires, Pabellón 2, Ciudad Universitaria, (1428) Buenos Aires, Argentina*
(Received 19 December 2003; revised manuscript received 9 July 2004)

Free energies of Rh-Pd alloys as functions of both temperature and composition are calculated using quasiharmonic lattice dynamics. The free energy of the disordered solid is determined from an ensemble of a large number of randomly generated configurations. Both configurational and vibrational contributions to the entropy and enthalpy of mixing are taken into account. We study the convergence with the number of random configurations, and analyze the validity of the zero static internal stress approximation (ZSISA), where only external strains are relaxed fully dynamically while internal stresses are relaxed in the static approximation. It is shown that the use of ZSISA allows an accurate calculation of free energies in a fraction of the time needed to carry out fully dynamic optimizations. From the values of free energies as functions of composition and temperature the phase diagram of Rh-Pd alloys is calculated, showing a good agreement with Monte Carlo simulations as well as with experiment. It is also shown that although free energies of mixing appear to be linear functions of temperature to a good approximation, the explicit expressions given by the configurational lattice dynamics method show that both enthalpies and entropies of mixing change appreciably with temperature.

DOI: XXXX PACS number(s): 63.50.+x, 63.20.Dj, 65.40.−b, 05.70.Ce

I. INTRODUCTION

The phase diagram of solids is essential in many applications, and the development of new methods to allow its calculation has been the scope of many research programs. The free energy is the key property to be determined as a function of both temperature and pressure. From the free energy, standard thermodynamic techniques can be used to build the corresponding phase diagrams.[1]

Marquez *et al.*[2] have recently used Monte Carlo simulations in the semigrand canonical ensemble (MCX) to obtain chemical potential differences as functions of both temperature and composition. To allow a proper sampling of configurational space these simulations were carried out considering explicit interchange of atoms. Free energy differences were obtained by integration of the calculated chemical potentials, and then used to construct the phase diagram of the Rh-Pd system. With this method, long runs are required to obtain chemical potentials with enough precision to allow a reliable determination of the phase diagram. In these simulations the interatomic potential was described within the embedded atom method (EAM) framework[3–5] with parameters fitted to *ab initio* calculations. The calculated phase diagram is in good agreement with experimental data. An important feature of the method is that it is applicable to any composition, sampling different arrangements of atoms and allowing for the local structural relaxation surrounding each atom. It was also shown that a mean field calculation is not adequate, at least for this system.

We note in passing that Hoyt *et al.*[6] have also used Monte Carlo simulations recently, for the phase diagram of the Cu-Pb system. Although they also used the EAM, the model parameters for the pure metals were taken from previous studies, while the Cu-Pb interaction was fitted to produce the experimental heats of mixing of Cu-Pb alloys. Another difference from the work of Marques *et al.* was that instead of calculating potential differences from a set of fixed compositions, Hoyt *et al.* fixed the chemical potential difference and then calculated the composition giving that difference. Although the method followed in these works is different both share in common the use of Monte Carlo simulations.

The Rh-Pd system has been studied previously using *ab initio* simulations and cluster expansions. Lu *et al.*[7,8] carried out simulations using the cluster-variation method (CVM) to calculate the phase diagram of Rh-Pd obtaining a consolute temperature of ≈1350 K. No local relaxation or vibrational effects were taken into account. Wolverton *et al.*[9] also used a generalized Ising model and effective pair and multisite interactions. By considering these effective interactions as explicit functions of volume it was possible to take into account the important effect of local relaxations though, again, vibrational contributions were not considered. Wang *et al.*[10] followed a different method using Monte Carlo simulations based on the embedded-cluster method. Though the calculated phase diagram is in fair agreement with the experimental determination of Shield and Williams,[11] local relaxations and vibrational effects were again not taken into account. However, and as mentioned by Wolverton *et al.*,[9] each one of these contributions may change the consolute temperature by approximately 200 K.

It is important to emphasize that, when possible, it is a general methodology in physics to corroborate the results given by one method with those given by different and independent methods. In this paper we propose the use of a very different method for calculating phase diagrams of alloys, namely configurational lattice dynamics (CLD). This method, used previously for ionic solid solutions,[12–14] is based on the generation of a large number of different atomic arrangements (configurations) on crystal lattice sites, fol-

lowed by quasiharmonic lattice dynamic optimization of each one of them. The optimization gives for each configuration not only the relaxed atomic positions but also its free energy, and hence, its statistical probability. The free energy of the mixed crystal is then obtained by averaging over the whole ensemble of configurations. Unlike MCX, CLD readily takes account of quantum effects, thus extending the range of application to lower temperatures. On the other hand, because of the basic assumption of small amplitudes of vibration, CLD is clearly not valid for the study of liquids, or even for solids at sufficiently high temperatures for the vibrations to be strongly anharmonic. The two methods are thus complementary. For this reason, we here illustrate the use of CLD by calculating the phase diagram of Rh-Pd alloys using exactly the same EAM potential as that previously used in the MCX simulations.[2]

In the following section we describe the basic equations of the configurational lattice dynamic method, and then we briefly describe the interatomic potential used. We first study the convergence of free energy values with the number of configurations and then we compare results using the zero static internal stress approximation (ZSISA),[15] where only external strains are relaxed fully dynamically while internal degrees of freedom are relaxed in the static approximation, with those obtained from fully dynamic optimizations. The results presented include enthalpies, entropies and free energies of mixing of Rh-Pd alloys and the corresponding phase diagram. An advantage of our method is that both vibrational and local relaxation contributions can be obtained directly, so allowing a quantitative assessment of their relative importance. In the conclusions we compare the results obtained with those obtained previously using Monte Carlo (MC) simulations, and comment on further possible applications of this method.

II. CONFIGURATIONAL LATTICE DYNAMICS

In the quasiharmonic approximation the free energy of a crystal, F, at a given temperature can be expressed as the sum of static and vibrational contribution

$$F = E_{\text{stat}} + F_{\text{vib}}(T). \tag{1}$$

E_{stat} is the potential energy of the static lattice and F_{vib} is the sum of harmonic vibrational contributions from all the normal modes

$$F_{\text{vib}} = \sum_{j=1}^{3N} \sum_{\mathbf{q}} \frac{1}{2}\hbar\omega_j(\mathbf{q}) + kT \ln(1 - e^{\hbar\omega_j(\mathbf{q})/kT}), \tag{2}$$

where the first term is the zero-point energy at $T=0$. For a macroscopic crystal the sum over $\mathbf{q}$ becomes an integral over a cell in reciprocal space, which can be evaluated by taking successively finer uniform grids until convergence is achieved.[16] The frequencies $\omega_j(\mathbf{q})$ are obtained by diagonalization of the dynamical matrix in the usual way[17]

$$\mathbf{D}(\mathbf{q})\mathbf{e} = \omega^2(\mathbf{q})\mathbf{e} \tag{3}$$

where $\mathbf{D}$ is defined by

$$D^{\alpha\beta}_{\kappa_i\kappa_j}(\mathbf{q}) = \frac{1}{\sqrt{m_{\kappa_i} m_{\kappa_j}}} \sum_{l_j} \Phi_{\alpha\beta}\begin{pmatrix} 0 & l_i \\ \kappa_i & \kappa_j \end{pmatrix} e^{i\mathbf{q}\cdot\mathbf{r}(l_j)}. \tag{4}$$

The $\Phi_{\alpha\beta}\left(\begin{smallmatrix} 0 & l_j \\ \kappa_i & \kappa_i \end{smallmatrix}\right)$ are second derivatives of the crystal energy with respect to atom coordinates

$$\Phi_{\alpha\beta}\begin{pmatrix} 0 & l_j \\ \kappa_i & \kappa_j \end{pmatrix} = \frac{\partial^2\Psi}{\partial x_\alpha\begin{pmatrix} 0 \\ \kappa_i \end{pmatrix} \partial x_\beta\begin{pmatrix} l_j \\ \kappa_j \end{pmatrix}}. \tag{5}$$

Here, $\mathbf{x}_\alpha\left(\begin{smallmatrix} l \\ \kappa \end{smallmatrix}\right)$ represents the α coordinate of the κth atom in the lth unit cell.

The most expensive task of a simulation is to determine the equilibrium structure. Once obtained, the evaluation of relevant thermodynamic properties is relatively fast. The vibrational frequencies entering in Eq. (2) do not depend on temperature explicitly, but do so implicitly through the position of the atoms in the unit cell and the lattice parameters which determines the dynamical matrix. The free energy thus obtained is a function of both the lattice parameters (a for a cubic crystal, a and c for a tetragonal crystal, etc.) and of the reduced coordinates which give the position of the atoms within the unit. The first and second sets of coordinates are often referred as external and internal coordinates, respectively. The whole collection of coordinates is denoted collectively as $\mathscr{R}$. For a given temperature and applied pressure, P_{ext}, the crystal structure is that which minimizes the availability $\tilde{G}$:[18]

$$\tilde{G}(\mathscr{R}) = F(\mathscr{R}) + P_{\text{ext}}V(\mathscr{R}^{\text{ext}}). \tag{6}$$

At the equilibrium configuration $P=P_{\text{ext}}$ and the availability equals the Gibbs energy

$$\tilde{G} = G \equiv F + PV. \tag{7}$$

We have described elsewhere a particularly efficient method to minimize $\tilde{G}$, allowing the study of unit cells with a large number of atoms,[19,20] and so no further details are presented here.

To find the equilibrium structure efficiently it is necessary to calculate not only the free energy but also its derivative with respect to both internal and external coordinates. For an ionic solid and using only two body potentials, only a few elements of the dynamical matrix are nonzero and this leads to a very efficient way of computing the derivatives of the free energy with respect to the whole set of coordinates. The many body forces characteristic of EAM potentials, on the contrary, makes the evaluation of the derivatives of the dynamical matrix much more expensive, the dynamical matrix now being less sparse than for ionic systems. For this reason we have resorted to ZSISA. In this approximation only the derivatives of the free energy with respect to the external coordinates are evaluated considering vibrational contributions, while the derivatives with respect to the internal coordinates are computed in the static approximation, so avoiding the evaluation of many dynamical matrix derivatives. Of course, a more self-consistent calculation involves the evaluation of the dynamical matrix with respect to the whole set of

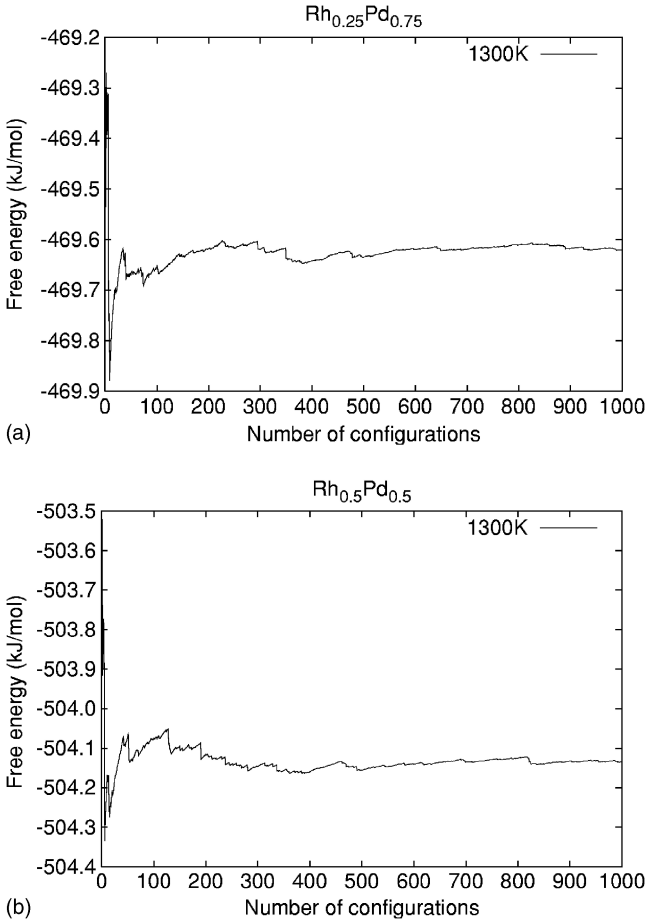

FIG. 1. Free energy as a function of the number of configuration at $T=1300$ K for (a) $Rh_{0.25}Pd_{0.75}$ and (b) $Rh_{0.5}Pd_{0.5}$. In these simulations we used unit cells with 32 atoms.

coordinates. For EAM potentials this is not only very expensive but the results produced do not differ significantly from those obtained using ZSISA, as shown in Fig. 2.

In the way outlined above one can obtain the relaxed structure of any given configuration. To simulate disordered solid alloys we use the CLD as proposed in Ref. 12. In this method one generates a set of configurations k, in each of which the location of the Rh (or Pd) atoms on sites within the unit cell is chosen at random. At each temperature a full dynamic optimisation of the structure of each configuration is then carried out, calculating at the same time several thermodynamic properties such as the Gibbs energy, G_k, the enthalpy, H_k and the entropy, S_k. The probability of each configuration is given by

$$p_k = \frac{\exp(-\beta G_k)}{\sum_k^K \exp(-\beta G_k)}, \tag{8}$$

where K is the total number of possible configurations for the supercell considered. The enthalpy of the disordered alloy is thus given by the ensemble average

$$H = \langle H_k \rangle = \sum_k^K p_k H_k. \tag{9}$$

The entropy, however, also contains a configurational term

$$S = \langle S_k \rangle - k_B \sum_k^K p_k \ln p_k \tag{10}$$

which leads to

$$G = -k_B T \ln K - k_B T \ln \left[\sum_k^K \exp(-\beta G_k)/K \right]. \tag{11}$$

Because it is in general not possible to carry out the summations in Eqs. (8) and (9) over all configurations, they are carried out over a subset K'. Consistently, K in the denominator of Eq. (11) is replaced by K'. The first term of Eq. (11) represents the contribution to G from the ideal entropy of mixing. Non ideal effects are included in the second term. Details of this method, and its application to ionic solids, were already published[12] and not repeated here.

III. INTERATOMIC POTENTIALS

In the EAM, the crystal energy per unit cell can be written as

$$E_{\text{stat}} = \sum_i F_i(\rho_i) + \tfrac{1}{2} \sum_i \sum_j {}' \phi_{ij}(r_{ij}), \tag{12}$$

where $F_i(\rho_i)$ is negative and represents the energy of "embedding" atom i in the electronic density ρ_i created by all other atoms in the crystal, and ϕ_{ij} is the core-core repulsion between atoms i and j, assumed to depend only on the type of the atoms i and j and the distance between them. The electron density ρ_i is assumed to be the sum of the electron densities of all other atoms at the nucleus of atom i:

$$\rho_i = \sum_j {}' f_j(r_{ij}), \tag{13}$$

where $f_j(r_{ij})$, assumed to be isotropic about atom j, is the electron density due to basis functions centered on atom j at a distance r_{ij}. The prime on the summations in Eqs. (12) and (13) indicates that terms with $r_{ij}=0$ are not included. The electronic densities are represented by simple exponential functions

$$f_j(r) = A_j \exp(-r/\sigma_j^{\text{e}}) \tag{14}$$

with different parameters A_j and σ_j^{e} (j=Rh,Pd) for each metal and with a cutoff of 6.0 Å. The repulsive potential is also assumed to have the simple form

$$\phi_{ij}(r) = B_{ij} \exp(-r_{ij}/\sigma_{ij}^{\text{r}}) \tag{15}$$

with different parameters B_{ij} and σ_{ij}^{r} for each type of interaction (Rh-Rh, Pd-Pd, and Rh-Pd). For the embedding energy we use

$$F_j(\rho_j) = -C_j \sqrt{\rho_j} \tag{16}$$

again, with different parameters C_j for each atom type. The model parameters are adjusted to reproduce the results of *ab initio* calculations and are reported in Ref. 2 and not repeated here. As seen in Figs. 1 and 2 of this work, the energies calculated with this potential are in very good agreement with the results of the *ab initio* simulations.

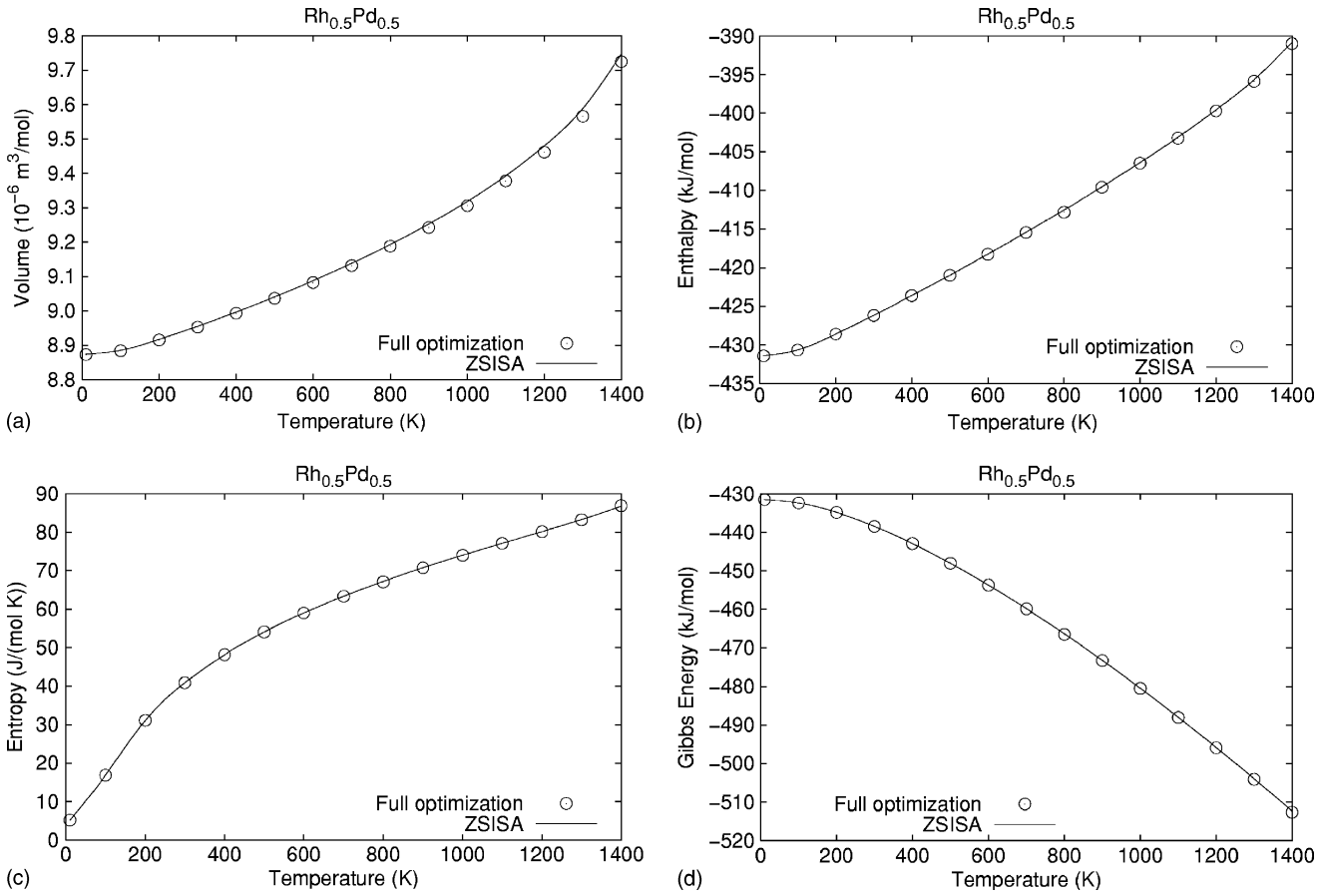

FIG. 2. Temperature dependence of several thermodynamic properties, using ZSISA and fully dynamic optimization, for (a) volume, (b) enthalpy, (c) entropy, and (d) Gibbs energy. We used a unit cell with 16 atoms of Rh and 16 atoms of Pd. Averages are calculated using 1000 configurations.

IV. RESULTS

The calculation of the phase diagram requires knowing the Gibbs energy as a function of both temperature and composition for a large number of these variables. For a given temperature and composition, the Gibbs energy is calculated from a large set of optimized configurations [Eq. (11)]. In order to carry out these calculations in a feasible amount of computing time we start by determining the number of configurations necessary to obtain suitable free energies. In Fig. 1 we show values of the Gibbs energy as a function of the number of configurations used in the ensemble, at $T=1300$ K for two different compositions and using a unit cell of 32 atoms. With 1000 configurations, free energies have converged by approximately 0.02 kJ/mol. Similar results were obtained for other temperatures as well as for cells with 108 atoms. All subsequent results presented here were done using 1000 configurations.

In order to save computer time we have also considered the zero static internal stress approximation[15] (ZSISA). In this approximation, only external degrees of freedom are relaxed fully dynamically, while all internal degrees of freedom are relaxed in the static approximation. In Fig. 2 we compare the results of the temperature dependence of several thermodynamic properties obtained using ZSISA with those obtained by carrying out fully dynamic optimizations. Because complete dynamic optimizations are very demanding in computer time we have done this comparison only for unit cells with 32 atoms. Here we considered a composition of $Rh_{0.5}Pd_{0.5}$, i.e., with 16 atoms of Rh and 16 atoms of Pd.

There is a very good agreement between the properties calculated using ZSISA and those obtained by fully dynamic optimizations. In Fig. 2 we compare the results for only some properties and a unit cell of $Rh_{16}Pd_{16}$; similar results were obtained for other thermodynamics properties and compositions. Thousands of configurations are necessary to calculate the phase diagram. For this reason and because the ZSISA approximation is much faster than fully dynamic optimizations, all subsequent calculations presented in this paper were consequently carried out using this approximation.

When using the ZSISA approximation, we found that the time required to carry out an optimization for cells with 32, 108, and 256 atoms scales approximately in the relation 1:17:640. Simulations using ZSISA, and for cells with 32 and 108 atoms are approximately 70 and 200 times faster than those with full dynamic optimizations. In comparison with MC simulations, the calculation of thermodynamic properties of mixing using CLD with 1000 configurations and unit cells of 108 atom takes approximately the same computer time as to carry out a 10^7+10^7

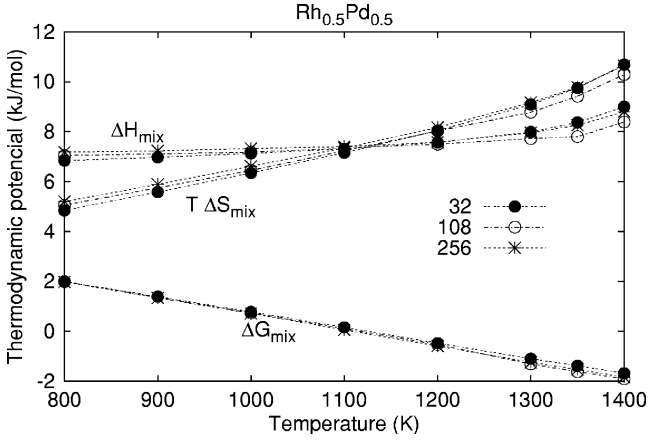

FIG. 3. Enthalpies, entropies (as $T\Delta S$) and Gibbs energies of mixing as functions of temperature for cells with 32, 108, and 256 atoms and a composition of $Rh_{0.5}Pd_{0.5}$ using ZSISA and fully dynamic optimizations. Averages were calculated using 1000 configurations.

(equilibration and production) run using MCX. For larger unit cells MCX simulations score favorably against the use of CLD.

To study the effect of the unit cell size on the calculated thermodynamic properties, we have carried out several calculations using unit cells with a total of 32, 108, and 256 atoms. In Fig. 3 we show the results of our simulations for a composition of $Rh_{0.5}Pd_{0.5}$, for temperatures between 800 and 1400 K. Similar results were obtained for other compositions. For temperatures higher than approximately 1300 K, both enthalpy and entropy values start to grow very fast as temperature is increased. This most likely unrealistic result is a clear indication of the breakdown of the quasiharmonic approximation. A careful examination of Fig. 3 shows that the quasiharmonic approximation starts to break down at slightly lower temperatures for the smaller unit cells. This is probably due to an artificial "stress" created by the smaller unit cells. For this reason and because the consolute temperature is near 1300 K (see Fig. 6), we have subsequently used only the results for $T \leqslant 1300\ K$. At $T=1300$ K the free energy of mixing of the 108-atom unit cell is converged, with respect to the 256-atom unit cell by better than 0.1 kJ/mol. This convergence is sufficient for the purpose of constructing the phase diagram and for this reason all subsequent calculations presented here were done using 108 atoms unit cells.

In passing, we note that the curve of ΔH_{mix} vs T for 32 atom unit cells given in Fig. 4 of Ref. 2 is in error as in that work the use of the minimum image convention precludes the use of these small cells.

In Fig. 4 we show the temperature dependence of free energies of mixing for two selected compositions. The lines are linear square fits to the calculated Gibbs energy values. Because of the linear trends, it would be tempting to assume that the intercepts should be ΔH_{mix} and that slopes should represent ΔS_{mix}, assuming that both functions are independent of temperature. However, and in spite that $\Delta G_{\mathrm{mix}}=a+bT$ (with a and b constants), both ΔH_{mix} and ΔS_{mix}

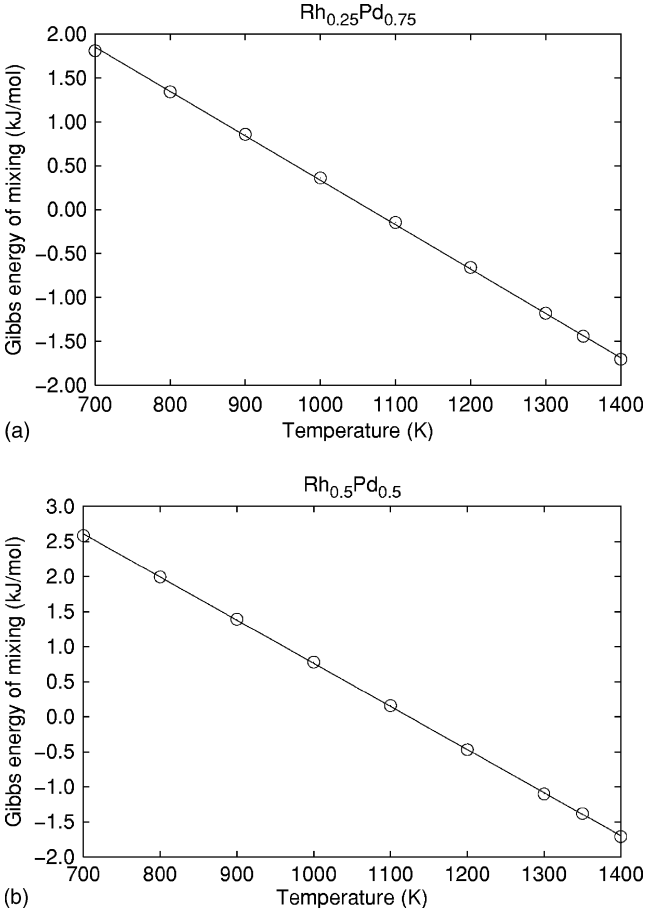

FIG. 4. Free energies of mixing vs temperature for two compositions. The line is a linear square fit to calculated free energy values.

depend slightly on temperature as illustrated in Table I. Values of ΔH_{mix} are calculated using Eq. (9) and values of ΔS_{mix} from those of ΔG_{mix} obtained from Eq. (11) and the previously calculated values of ΔH_{mix}. So, and in spite that free energies of mixing appear to vary linearly with temperature, the explicit expressions given by CLD show that enthalpies and entropies of mixing change appreciably with temperature.

Once ΔG_{mix} is known as a function of both temperature and composition, is it possible to build the corresponding binodal curve using the standard common tangent construction.[1] In Fig. 5 we illustrate this method for a temperature of 1000 K, well below the consolute temperature, and for $T=1300$ K, which is close to this transition temperature. From the positions of the intersections of the tangents with the ΔG_{mix} vs T curves it is then straightforward to build the binodal curve presented in Fig. 6. This curve has been built by using the tangent construction at $T=800$, 900, 1000, 1100, 1200, and 1300 K, and fitting these data to an equation of the form

$$T(x_{\mathrm{Rh}}) = a + b \ln x_{\mathrm{Rh}} + c \ln(1 - x_{\mathrm{Rh}}) + d x_{\mathrm{Rh}}(1 - x_{\mathrm{Rh}}). \tag{17}$$

In Fig. 6 we have plotted also the phase diagram obtained using MC simulations which is a completely different

TABLE I. Temperature dependence of the enthalpy and entropy of mixing for two compositions and at a few selected temperatures. "Linear fit" values represent the intercept and slope of ΔG_{mix} vs T assuming ΔH_{mix} and ΔS_{mix} independent of T, a common assumption not supported by our calculations.

	ΔH_{mix} (kJ mol^{-1})				ΔS_{mix} (J mol^{-1} K^{-1})			
	Linear fit	900 K	1100 K	1300 K	Linear fit	900 K	1100 K	1300 K
$Rh_{0.25}Pd_{0.75}$	5.39	5.34	5.61	6.02	5.06	4.99	5.23	5.54
$Rh_{0.5}Pd_{0.5}$	6.91	6.97	7.31	7.99	6.15	6.20	6.51	6.99

method. We also show the spinodal curve obtained from both methods. The spinodal limits the region of T-x where solid solutions are kinetically as well as thermodynamically unstable. For a given temperature, the compositions that define the spinodal are those for which $\partial^2 G_{\mathrm{mix}}/\partial x^2 = 0$.

Both MC and CLD calculations agree very well with the experimental data, as presented in Fig. 7 of Ref. 2, and not repeated here. There is also a good agreement between the results obtained from both methods. The MC simulations predicted a consolute temperature of about 1300 K while the present simulations indicate a temperature slightly below 1400 K. This relatively small difference can in principle be attributed to two different approximations. First, classical Monte Carlo simulations neglect quantum effects. While for some systems it was found that quantum effects are not negligible even at relatively high temperatures,[21] we have checked that the neglect of these effects in our lattice dynamic simulations do not change the results presented in this paper, at least on the scale of the graphs presented here. Second, the other main approximation is the neglect of further anharmonic terms by quasiharmonic approximation. As we mentioned above, it seems that the quasiharmonic approximation starts to break down at $T \approx 1400$ K, and indeed the simulations give many imaginary frequencies at $T \approx 1450$ K and above. In conclusion, it seems that the relatively small difference between the results of both methods is the neglect of further anharmonic terms in the quasiharmonic approximation.

While CLD provides directly absolute values of both enthalpies and entropies of mixing, MCX simulations yield primarily enthalpies of mixing. For this reason, a common assumption has been the use of the "ideal" entropy of mixing

$$\Delta S_{\mathrm{mix}}^{\mathrm{ideal}} = R\{x \ln x + (1-x)\ln(1-x)\} \tag{18}$$

to calculate approximate free energies of mixing (as $\Delta G_{\mathrm{mix}}^{\mathrm{ideal}} = \Delta H_{\mathrm{mix}} - T\Delta S_{\mathrm{mix}}^{\mathrm{ideal}}$). The use of this approximation is illustrated in Fig. 7 where we show the free energy of mixing

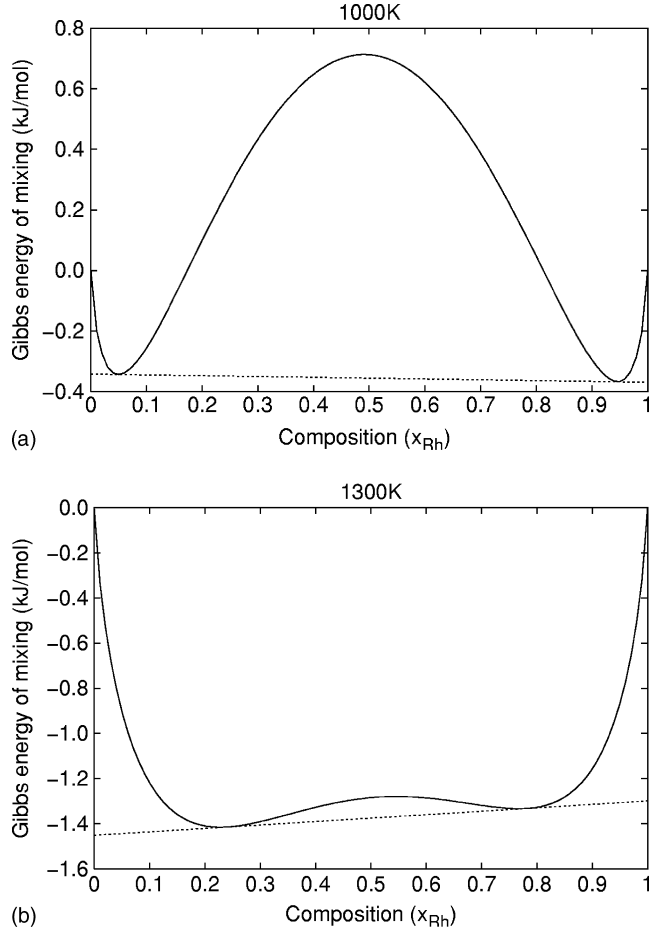

FIG. 5. Free energy of mixing vs composition at (a) 1000 and (b) 1300 K. The intersections of the common tangents with the ΔG_{mix} curves are used to construct the phase diagram given in Fig. 6.

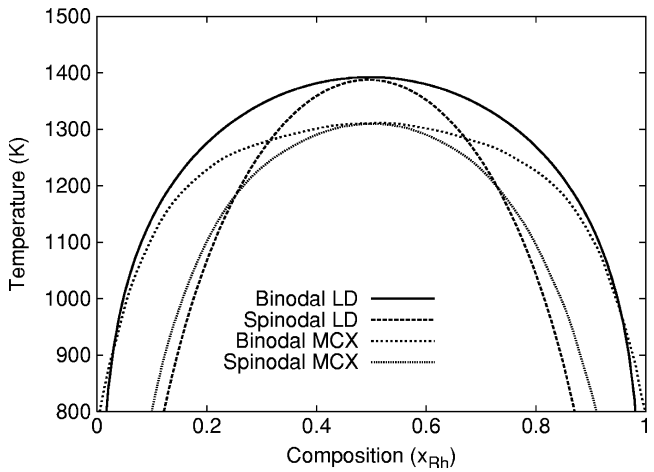

FIG. 6. Calculated phase diagram of Rh-Pd alloys using configurational lattice dynamics (LD) and semigrand canonical Monte Carlo simulations (see Ref. 2) (MCX).

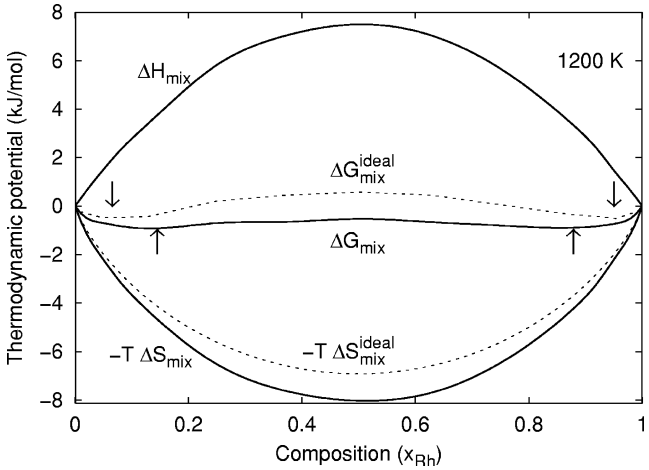

FIG. 7. Free energy, enthalpy, and entropy of mixing of Rh-Pd alloys at 1200 K. Arrows indicate the points where the common tangent intersects the ΔG_{mix} curves and which define the spinodal given in Fig. 6. Also shown is the ideal entropy of mixing ($\Delta S_{\mathrm{mix}}^{\mathrm{ideal}}$) and $\Delta G_{\mathrm{mix}}^{\mathrm{ideal}}$ calculated as $\Delta G_{\mathrm{mix}}^{\mathrm{ideal}}=\Delta H_{\mathrm{mix}}-T\Delta S_{\mathrm{mix}}^{\mathrm{ideal}}$.

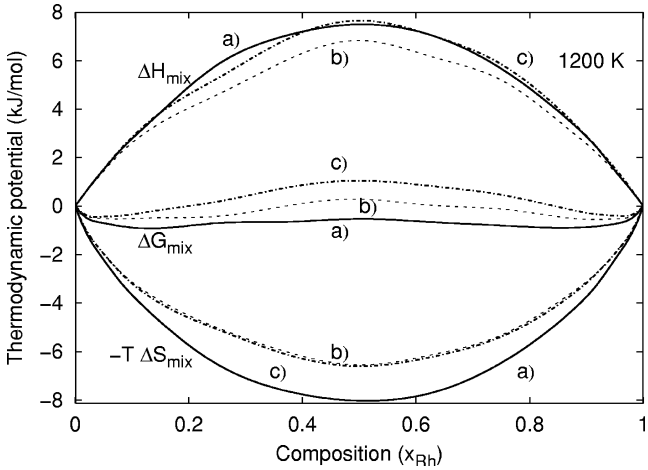

FIG. 8. Free energy, enthalpy, and entropy of mixing of Rh-Pd alloys at 1200 K for three different sets of simulations: (a) full calculations including vibrations and relaxations, (b) without vibrations and with relaxations, and (c) without vibrations and without relaxations.

at 1200 K decomposed in its contributions ΔH_{mix} and $-T\Delta S_{\mathrm{mix}}$, using values of entropies of mixing with and without this approximation. The arrows indicate the positions where a common tangent construction would give the compositions, at $T=1200$ K, of the binodal curve of the phase diagram. It is easily seen that the use of this ideal entropy of mixing has a very important effect on the calculated phase diagram, not justifying its use, at least for this system.

Another common assumption in MCX simulations has been the neglect of local relaxation, vibrational contributions or both of them. To study the importance of vibrational and relaxation effects we have repeated our simulations using CLD for different cases. In the first, vibrational contributions were neglected, i.e., we carried out only static simulations, but allowing the atoms to relax. In the second case, both vibrations and relaxation were not taken into account. The results of this simulations at 1200 K are shown in Fig. 8, where we have three different cases: (a) with vibrations and relaxations, (b) without vibrations and with relaxation, and (c) without vibrations and without relaxation. Enthalpies of mixing for case (b) are systematically below those of case (a) because the neglect of vibrational contributions, with a maximum difference of about 1 kJ/mol at $x_{\mathrm{Rh}}\approx 0.5$. The curve for case (b), which neglects vibrations, is below that of case (c) because of the extra stability provided by local relaxations. The curve for cases (a) (both effects taken into account) and case (c) (both effects not taken into account) are very similar except at $x_{\mathrm{Rh}}\approx 0.3$. We can see that, for this system, vibrational and relaxation effects on enthalpies of mixing mostly cancel to each other. A similar study can be done for the entropies of mixing. Comparing cases (b) and (c) it can be seen that relaxations do not play an important role in the entropies of mixing. On the contrary, and by comparison of cases (a) and (b), we see that vibrations are very important changing the values of $-T\Delta S_{\mathrm{mix}}$ by as much as approximately 1.5 kJ/mol at $x_{\mathrm{Rh}}\approx 0.5$.

V. CONCLUSIONS

In this paper we have used CLD and an EAM potential to calculate the phase diagram of Rh-Pd alloys, which is in very good agreement with experimental data and results obtained from MC simulations. This method provides not only an alternative to MC simulations but a method to determine directly absolute values of free energies, enthalpies and entropies of mixing. Values of these quantities can be obtained also from MC simulations but only indirectly by integration of chemical potentials.[2] We have shown that vibrational and relaxation contributions to enthalpies of mixing almost cancel to each other, though none of these effects is negligible. On the contrary, relaxation effects do not seem to play an important role on entropies of mixing, though vibrational effects can change entropies of mixing by $\approx 20\%$ at $x_{\mathrm{Rh}}\approx 0.5$ and 1200 K.

We have studied the convergence of free energy values with the number of configurations and showed that suitable values of free energies can be obtained from simulations with 1000 configurations. We have showed also that, at least for this system, ZSISA provides an excellent approximation to fully dynamic optimizations in a fraction of the computer time.

Though free energies of mixing appeared to be linear functions of temperature to a good approximation, explicit expressions for both enthalpies and entropies of mixing reveal that contrary to the common approximation of considering them as constant they both vary with temperature. For $Rh_{0.25}Pd_{0.75}$ and T between 900 and 1300 K, for instance, ΔH_{mix} and $-T\Delta S_{\mathrm{mix}}$ vary by approximately 12% and 11%, respectively. Getting these quantities from a liner fit to ΔG_{mix} is thus insensitive and involves considerable error.

The proposed method should prove particularly useful at low temperatures where the neglect of quantum effects in classical MC and molecular dynamics (MD) simulations

would prevent the use of these methods. An example is the calculation of heat capacities of disorder solids at very low temperatures where recent experimental measurement on Cu_3Au alloys[22] have shown an anomalous peak at $T \approx 70$ K. Work on this area in currently in progress.

ACKNOWLEDGMENTS

This work was supported by Grant No. BID 802/OC-AR PICT 0361 from ANPCyT. GDB acknowledges support from el Consejo Nacional de Investigaciones Científicas y Técnicas de la República Argentina.

[1] A. Putnis, *Introduction to Mineral Sciences* (Cambridge University Press, Cambridge, 1992).
[2] F. M. Marquez, C. Cienfuegos, B. K. Pongsai, M. Yu. Lavrentiev, N. L. Allan, J. A. Purton, and G. D. Barrera, Modell. Simul. Mater. Sci. Eng. **11**, 115 (2003).
[3] M. Daw and M. Baskes, Phys. Rev. B **29**, 6443 (1984).
[4] M. W. Finnis and J. E. Sinclair, Philos. Mag. A **50**, 45 (1984).
[5] F. Ercolessi, M. Parrinello, and E. Tosatti, Philos. Mag. A **58**, 213 (1988).
[6] J. J. Hoyt, J. W. Garvin, E. B. Webb III, and M. Asta, Modell. Simul. Mater. Sci. Eng. **11**, 287 (2003).
[7] Z. W. Lu, S.-H. Wei, and A. Zunger, Phys. Rev. Lett. **66**, 1753 (1991).
[8] Z. W. Lu, B. M. Klein, and Z. Zunger, J. Phase Equilib. **16**, 36 (1995).
[9] C. Wolverton, D. de Fontaine, and H. Dreyssé, Phys. Rev. B **48**, 5766 (1993).
[10] Y. Wang and J. S. Faulkner, Phys. Rev. Lett. **70**, 3287 (1993).
[11] J. E. Shield and R. K. Williams, Scr. Metall. **21**, 1475 (1987).
[12] N. L. Allan, G. D. Barrera, R. M. Fracchia, M. Yu. Lavrentiev, M. B. Taylor, I. T. Todorov, and J. A. Purton, Phys. Rev. B **63**, 094203 (2001).
[13] N. L. Allan, G. D. Barrera, M. Y. Lavrentiev, I. T. Todorov, and J. A. Purton, J. Mater. Chem. **11**, 63 (2001).
[14] N. L. Allan, G. D. Barrera, R. M. Fracchia, B. K. Pongsai, and J. A. Purton, J. Mol. Struct.: THEOCHEM **506**, 45 (2000).
[15] N. L. Allan, T. H. K. Barron, and J. A. O. Bruno, J. Chem. Phys. **105**, 8300 (1996).
[16] At very low temperatures special procedures are required. See, e.g., J. A. O. Bruno, N. L. Allan, and T. H. K. Barron, J. Phys.: Condens. Matter **12**, 549 (2000).
[17] D. C. Wallace, *Thermodynamic of Crystals* (Wiley, New York, 1972).
[18] A. B. Pippard, *The Elements of Classical Thermodynamics* (Cambridge University Press, Cambridge, 1964).
[19] G. D. Barrera and R. H. de Tendler, Comput. Phys. Commun. **105**, 159 (1997).
[20] E. P. Isoardi, N. L. Allan, and G. D. Barrera, Phys. Rev. B **69**, 024303 (2004).
[21] R. M. Fracchia, G. D. Barrera, N. L. Allan, T. H. K. Barron, and W. C. Mackrodt, J. Phys. Chem. Solids **59**, 435 (1998).
[22] L. J. Nagel, L. Anthony, and B. Fultz, Philos. Mag. Lett. **72**, 421 (1995).